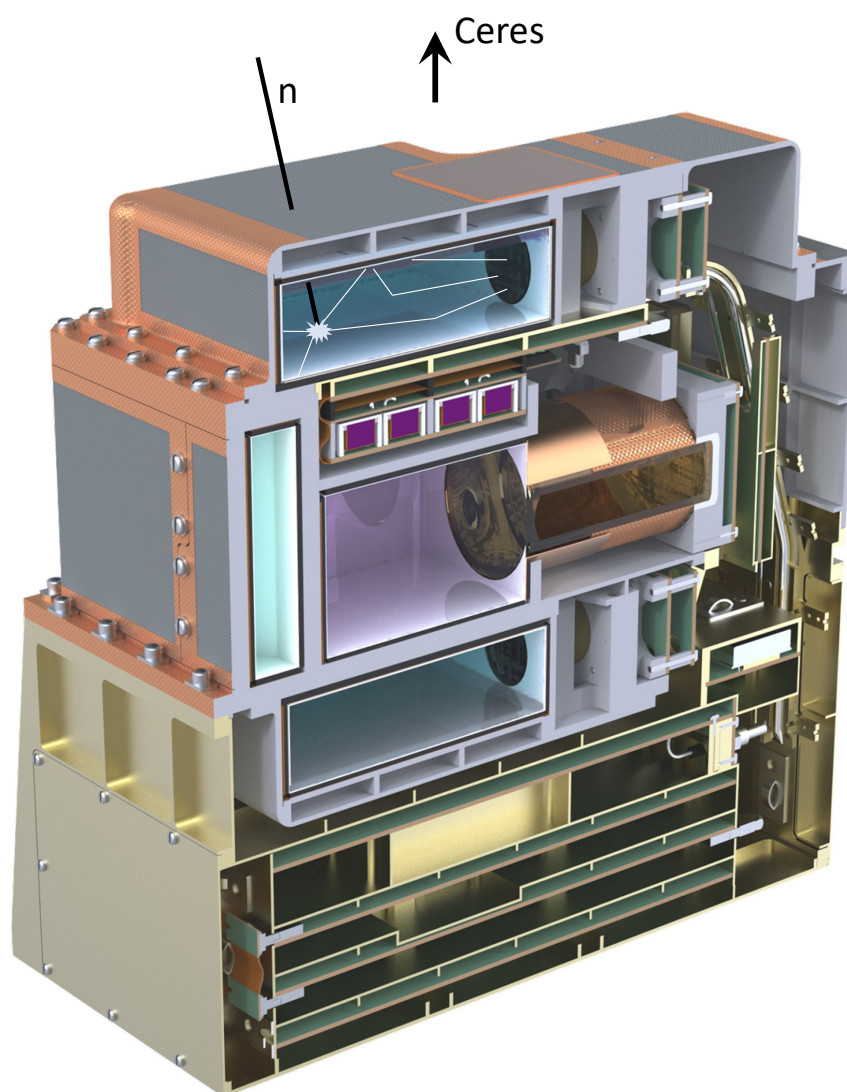# DAWN'S GAMMA RAY AND NEUTRON DETECTOR (GRAND)

INSTRUMENT DESCRIPTION

Ceres

n

Cutaway view of the GRaND instrument and neutron interaction with a scintillator [1]. Instrument artwork by S. Storms, Los Alamos National Laboratory.

Version 2.0 — Based on the PDS3 instrument catalog
Thomas H. Prettyman
Planetary Science Institute
8-Feb-2021

CONTENTS

ACRONYMS AND ABBREVIATIONS

ADC	Analog to Digital Converter
ATLO	Assembly, Test, and Launch Operations
BGO	Bismuth Germanate
BLP	Boron-loaded plastic
CAT	Event Category
CPT	Comprehensive Performance Test
CZT	Cadmium Zinc Telluride
FPGA	Field Programmable Gate Array
FWHM	Full-Width-at-Half-Maximum
GRaND	Gamma Ray and Neutron Detector
keV$_{ee}$	Charged particle electron-equivalent energy
Li-glass	Lithium-loaded glass
MCA	Mars Closest Approach
NAIF/SPICE	Software package for calculating the position and orientation of the spacecraft maintained by the Navigation and Ancillary Information Facility at the NASA Jet Propulsion Laboratory
S/C	Spacecraft
SCLK	Spacecraft clock ticks (s)
TELREADOUT	Length of each science accumulation interval (s)
TELSOH	Sampling interval for the state of health telemetry (s)
X(a,b)Y	Nuclear reaction shorthand notation, equivalent to a + X $\rightarrow$ Y + b. The residual nucleus Y is sometimes implied, e.g. for ^{10}B(n,α) the residual nucleus is ^{7}Li*, and the target X can be omitted to indicate a generic reaction, e.g. (n,γ).

INTRODUCTION

The Dawn Mission's Gamma Ray and Neutron Detector (GRaND) collected data that can be used to measure and globally map the subsurface elemental composition of (1) Ceres and (4) Vesta [2-10]. **For a detailed description of GRaND see [1].** This document provides a brief overview of GRaND to accompany the PDS4 data set. Additional details on instrument performance, operations and processing procedures required to use the data can be found in documents accompanying this archive.

GRaND measured the spectrum of planetary gamma rays and neutrons produced by cosmic ray interactions and the decay of radioelements within the regolith while in orbit around Dawn's primary targets. Planetary radiation emissions were also observed during a close flyby of Mars. The instrument, which is mounted on the +Z deck of the spacecraft, consists of 21 sensors designed to separately measure radiation originating from the surface of each asteroid and background sources, which include solar energetic particles and cosmic ray secondary particles produced in the spacecraft and instrument. The nuclear spectroscopy data provided by GRaND can be analyzed to determine the abundance of major elements, such as O, Mg, Si, Al, Ca, and Fe found in silicate minerals and aqueous alteration products; incompatible elements, including K and Th, detected by gamma ray emissions from the decay of long-lived radioisotopes; and H and C found in aqueous alteration products, organic matter and water ice.

PLANETARY NUCLEAR SPECTROSCOPY — BASICS

Introductory materials on planetary nuclear spectroscopy theory, instrumentation, methods, and missions are provided in the literature [e.g., 11,12,13]. The basics are summarized here.

Nuclear spectroscopy is used to determine the elemental composition of planetary surfaces and atmospheres. Radiation, including gamma rays and neutrons, is produced steadily by cosmic ray bombardment of the surfaces and atmospheres of planetary bodies and by the decay of radionuclides in the regolith (Fig. 1). The leakage flux of gamma rays and neutrons contains information about the abundance of major elements, selected trace elements, and ice constituents (e.g., H, C, and N) as well as elements associated with aqueous alteration products such as Cl. Gamma rays and neutrons can be measured at altitudes less than a planetary radius, enabling global mapping of elemental composition by an orbiting spacecraft. Radiation that escapes into space originates from shallow depths (< 1 m within the solid surface). Consequently, nuclear spectroscopy is complementary to other surface mapping techniques, such as reflectance spectroscopy, which is used to determine the mineralogy of planetary surfaces. The main benefit of gamma ray and neutron spectroscopy is the ability to reliably identify elements important to planetary geochemistry and to accurately determine their abundance. This information can be combined with other remote sensing data, including surface thermal inertia and mineralogy, to investigate many aspects of planetary science.

Nuclear reactions and radioactive decay result in the emission of gamma rays with discrete energies, which provide a fingerprint that can uniquely identify specific elements in the surface. Depending on the composition of the surface, the abundance of major rock-forming elements such as O, Mg, Al, Si, Cl, Ca, Ti, Fe, as well as Cl, a tracer of aqueous alteration, H, and long-lived elements with radioisotopes (^{40}K, U series, Th series) can be determined from measurements of the gamma ray spectrum when they are present in detectable quantities. High

energy neutrons produced by cosmic ray interactions lose energy in successive collisions with nuclei in the regolith, and are ultimately absorbed or escape into space. Their sensitivity to elemental composition depends on three main types of reactions that are important in three broad energy ranges measured by GRaND: inelastic scattering (important for fast neutrons greater than about 0.7 MeV); elastic scattering (epithermal neutrons between 0.1 eV to 0.7 MeV); and absorption (thermal neutrons less than 0.1 MeV). Fast neutrons are sensitive to the average atomic mass of the regolith when H is present in small quantities (H weight fractions less than a few hundred ppm). Epithermal neutrons are sensitive to the abundance of H and are relatively insensitive to variations in the abundance of major elements. Thermal neutrons are sensitive to strong absorbers such as Fe, Ti, N, Cl, Gd, and Sm.

Close proximity to the planetary body is needed to measure neutrons and gamma rays because their emission rate is very low, for example, to reflected sunlight. Sensors used for gamma ray and neutron spectroscopy are generally insensitive to incident direction. Consequently, spatial resolution depends on orbital altitude, and higher resolution can be achieved by moving closer to the planet. Measurements of large regions (usually on the scale of 100s of km) are generally made using nuclear spectroscopy, in contrast to the meter to kilometer scale generally achieved by reflectance and thermal-emission spectroscopy. As a rough guide, a nuclear spectrometer can resolve distinct, sources of radiation on planetary surfaces that are separated by an arc length of about 1.5 times the orbital altitude of the spacecraft. For the 210-km mean altitude achieved by Dawn at Vesta, the spatial resolution was about 300-km, which is smaller in scale than the 500-km diameter Rheasilvia basin. During Dawn's final mission phase, the spacecraft was placed in an eccentric orbit, with altitudes as low as 35 km, with a spatial resolution of about 50 km. This enabled elemental analyses of smaller-scale geologic units, including the 90-km diameter Occator crater.
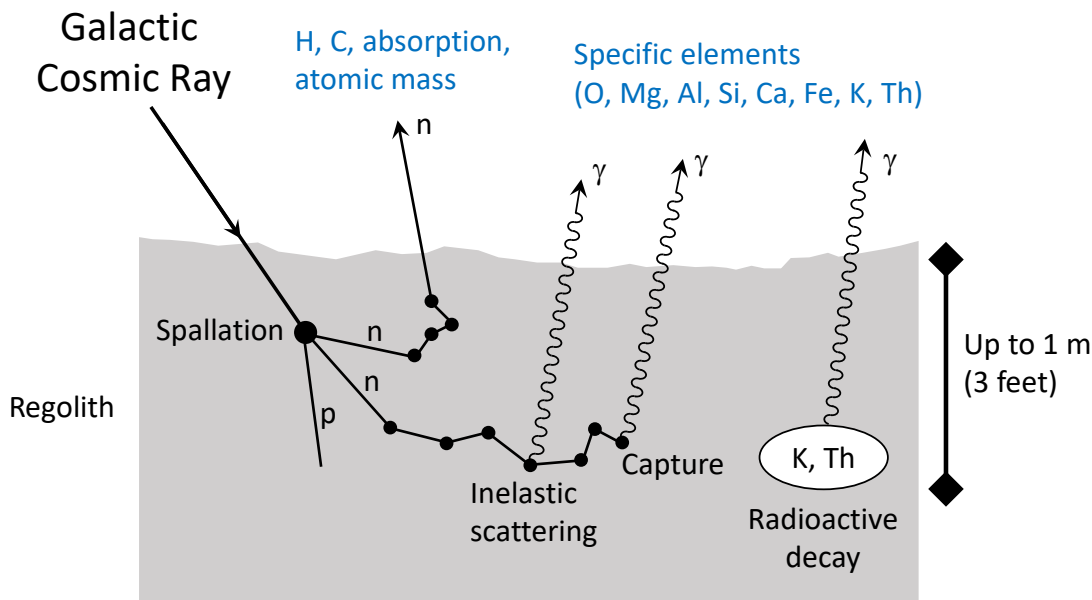

Figure 1. *Splat!* The interaction of a galactic cosmic ray ion with nuclei in the surface of a planetary body produces a spray of secondary particles, including neutrons (n) and protons (p). The secondaries and their progeny undergo successive collisions some of which produce gamma rays (γ). Gamma rays are also made by the decay of natural radioelements present in silicate minerals. Radiation that escapes the surface can be measured by an orbiting nuclear spectrometer and provides a chemical fingerprint of the subsurface to depths of <1 m [11].

GRAND SCIENCE

Some examples of science investigations that can be carried out with the data acquired by GRaND include:

- Provide geochemical data needed to constrain the thermal evolution of Vesta and Ceres and to determine the role of water in their development.
- Determine the composition of the primordial solar nebula as a function of heliocentric distance. For example, measure the K/Th ratio to determine the proportion of volatile to refractory elements in the source material from which Vesta and Ceres accreted.
- Constrain the interior composition of Vesta and Ceres by measuring stratigraphic variations within large impact basins that probe the deep interior (for example, the large, south-polar basin on Vesta).
- Determine possible origins of near-surface hydrogen on Vesta and determine the depth of the ice table with latitude on Ceres.
- At Vesta, determine the relationship between compositional terranes and howardite, eucrite and diogenite (HED) meteorites. Is the chemistry of Vesta more diverse than suggested by the HEDs?
- At Ceres, characterize the products of aqueous alteration (brines and residues) to constrain interior structure and crustal evolution.

The data can also be used to support investigations in other areas of space science, including cosmic ray physics, space physics, and astrophysics. The Dawn mission spanned 11 years in flight, acquiring data in interplanetary space during cruise, and at Dawn's planetary targets. During this time, GRaND observed galactic cosmic rays, solar energetic particles, solar flare X-rays, gamma-ray bursts, and acceleration of electrons at Ceres' bow shock. Bursts of energetic electrons observed at Ceres are thought to result from the interaction of the solar wind with a transient atmosphere [14].

CALIBRATION

Calibration data for GRaND was acquired during assembly, test, and launch operations (ATLO), before and after delivery of the instrument for integration with the spacecraft, and during flight [1]. Prior to delivery, the instrument was characterized at a calibration facility at Los Alamos National Laboratory and on the bench using neutron and gamma ray sources. The main goals of the calibration exercise were to:
- verify the functionality of each of the sensors;
- determine the energy calibration for each sensor and event category;
- determine the absolute calibration (relationship between flux and counting rate) for each sensor and event category as a function of incident energy and direction.

Data acquired during comprehensive performance tests (CPTs) following integration of GRaND with the spacecraft provide supplemental information needed to confirm the energy calibration. Following launch, GRaND was operated during Earth-Mars cruise to measure the response to galactic cosmic rays and energetic particles in the space environment. The data are needed to characterize background sources (for example, prompt neutron and gamma production by galactic cosmic ray interactions with the bulk spacecraft and the buildup of induced radioactivity within the sensor).

In addition, GRaND acquired data during Mars Closest Approach (MCA), which was compared directly to data acquired by 2001 Mars Odyssey, enabling cross-instrument calibration of GRaND during flight, providing bounds on

the concentration of hydrogen on Vesta [2]. The relationship between particle energy and measured pulse height depends on bias voltage settings and environmental factors, such as the temperature of the scintillator, which can vary with time. During flight, prominent gamma ray and neutron spectral features with known energies are used to determine time-dependent, energy calibration parameters.
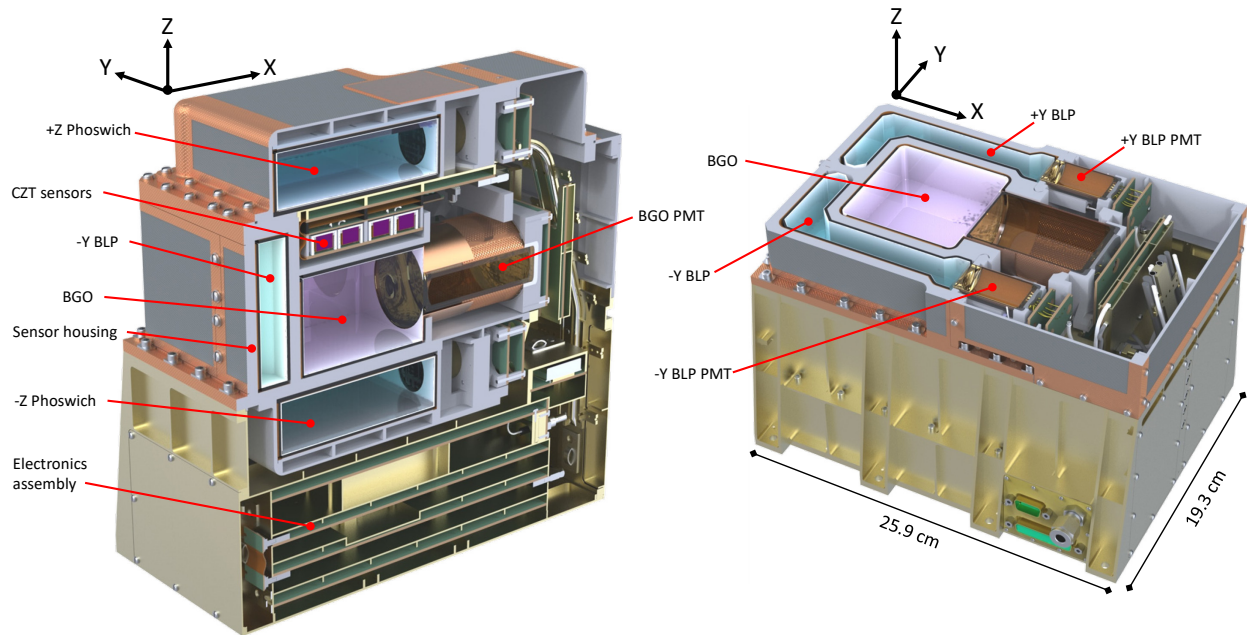

Figure 2. Cutaway views of GRaND showing the location of sensors. The coordinate system is the same as that of the spacecraft (Fig. 2). Photomultiplier tubes (PMTs) that read out the scintillators are on the +X (PX) side of the instrument. During science mapping, the center of the target (Vesta or Ceres) was in the +Z (PZ) direction. Artwork adapted from [1].

SENSORS

GRaND used scintillator- and semiconductor-based radiation sensors to detect neutrons and gamma rays as well as energetic particles from the space environment. A scintillator is a transparent material that converts the kinetic energy of charged particles (such as electrons produced by gamma ray interactions or alpha particles and recoil protons produced by neutron reactions) into flashes of light detectable by a photosensor, such as a photomultiplier tube. Semiconductors can also be used to detect gamma rays. Swift electrons produced by Compton and photoelectric interactions ionize the semiconductor, producing electron-hole pairs. The electrons and holes drift under the influence of an applied electric field to electrical contacts. As they drift, the electrons and holes induce charge on contacts, which can be measured by a charge-sensitive preamplifier. The amplitude of the charge pulse is proportional to the energy deposited by the gamma ray, which enables semiconductors to be used for spectroscopy.

The sensors and shielding/structural materials were arranged in order to separately measure gamma rays and neutrons originating from the target body from background sources, including neutrons and gamma rays produced

by cosmic rays in the bulk spacecraft, and energetic particle interactions with the instrument. The sensors on GRaND were selected to operate between -20°C and 30°C and do not require active cooling.

GRaND uses four types of radiation sensors:

1. **Bismuth germinate (BGO) scintillator**: A 7.6 (X) cm x 7.6 (Y) cm x 5.08 (Z) cm BGO crystal (approximately 300 cm^3 volume) is located in the center of the scintillator subassembly. The scintillator is coupled to a 5.08-cm diameter photomultiplier tube. BGO has high density and high atomic number and is sensitive to gamma rays over a wide energy range (up to 10 MeV). The pulse height resolution at room temperature is approximately 10% full-width-at-half-maximum (FWHM) at 662 keV.

2. **Cadmium Zinc Telluride (CZT) semiconductors**: CZT was a demonstration technology on Dawn. A planar array of 4x4 CZT crystals is positioned on the +Z side of the BGO crystal (Fig. 1), which faces towards the target body center during science mapping. Each crystal is 10 mm x 10 mm x 7 mm. Consequently, the array has a sensitive volume of about 11 cm^3. Coplanar electrode grids are used to mitigate the effects of hole trapping, resulting in excellent peak shape and pulse height resolution over a wide range of energies. The pulse height resolution during ground calibration was better than 3% FWHM at 662 keV, and the array was designed to measure gamma rays with energies up to 3MeV. The relatively high energy resolution of the CZT array enabled accurate measurement of gamma rays in the densely-populated, low energy region of the spectrum, which contains gamma rays from radioactive decay and cosmic-ray induced reactions within the surface of the target planetary body. While the CZT array achieved engineering goals during flight, including demonstration of annealing, aspects of its performance following launch were anomalous. As a result, the data from this sensor were not used in early science studies.

3. **B-loaded plastic (BLP) scintillator**: Two L-shaped boron-loaded plastic (BLP) scintillators (each 193 cm3) are located on the -Y and +Y sides, surrounding the sides of the BGO crystal and CZT array. The scintillators act as anticoincidence shields to reject cosmic ray interactions. In addition, the scintillators are sensitive to neutrons. Fast neutrons (with energies greater than 700 keV) can undergo elastic scattering with H within the plastic to produce knock-on protons, which ionize the scintillator, resulting in the production of detectable light. In addition, thermal and epithermal neutrons can be captured via the $^{10}B(n,\alpha)^7Li^*$ to produce 93 keV$_{ee}$ light output. Note that the subscript 'ee' indicates an electron-equivalent energy, corresponding to the energy a swift electron would need to produce the same light output as the reaction products. Deexcitation of the reaction product 7Li* produces a 478 keV prompt gamma ray. Fast neutrons with energies greater than about 700 keV produce a characteristic double pulse signature, corresponding to light output from fast-neutron proton recoils followed later by neutron capture with ^{10}B after the neutron has thermalized. The amplitude of the first pulse is related to the energy of the incident neutron. Thermal and epithermal neutrons also produce a unique coincidence signature, corresponding to 93 keV of light produced in the plastic in coincidence with 478 keV deposited in the BGO crystal.

4. **Li-glass, B-loaded-plastic phosphor sandwich (phoswich)**: Two BLP scintillators are located on the nadir (-Z) and spacecraft (+Z) sides of the instrument, centered on the CZT array and BGO crystal. Each BLP scintillator is approximately 10.16 cm x 10.16 cm x 2.54 cm (264 cm^3) and is read out by a 2.54 cm diameter phototube. With the exception of the outward facing side, each scintillator is covered with a sheet of Gd foil, which absorbs thermal neutrons. The outward facing side is covered by a plate of lithium-loaded glass, 0.2 cm thick. The lithium-loaded glass is optically-coupled to the BLP such that the phototube measures light produced in both the glass and the plastic. ^6Li is a strong thermal neutron absorber. Consequently, the BLP is shielded from thermal neutrons. Epithermal neutrons that undergo capture via the $^{10}B(n,\alpha)$ reaction in the BLP produce 93 keV$_{ee}$ light output. Thermal and epithermal neutrons can undergo neutron capture via the $^6Li(n,t)$ reaction, which produces

approximately 340 keV$_{ee}$, which is seen as a separate peak in the pulse height spectrum. Consequently, the thermal neutron signature can be determined by weighted difference between the counting rates observed for the two reactions. The spectrum of fast neutrons is measured using the double pulse signature in the BLP. In addition, the (n,γ) BLP-BGO coincidence signature provides an independent, low background measurement of epithermal neutrons.

ELECTRONICS

GRaND derived power from the S/C 28Vdc power bus. The instrument low voltage power supply provided ±5V to the digital and analog circuits and +12V to the high voltage power supply, which supplied 0 to +1500V to the photomultiplier tubes and -1500V/+70V to the CZT sensors. The instrument transmitted and received data through an RS-422 interface. The instrument was controlled by a UTMC micro-controller, which managed instrument subsystems, processed commands, monitored state of health (SOH), and processed the science data. Each of the radiation sensors was read out by analog front-end electronics, which provided shaped pulses, which were digitized by analog-to-digital-converters (ADC) to determine pulse amplitude, and timing signals for analysis of coincident events. Signals from the FEE were processed by an Actel field-programmable-gate-array (FPGA). The FPGA categorized signals from the sensors, identifying patterns corresponding to important events. The event categories are described in the Measured Parameters section. SOH data were recorded in the engineering telemetry, including high voltage values and temperatures. Commandable parameters included instrument high voltage settings, parameters used to classify coincidence events, and measurement intervals.

ACCOMMODATION

GRaND was mounted on the +Z deck of the spacecraft (SC), offset from the center of the spacecraft in the (+X,+Y) quadrant (Fig. 3). The placement and orientation (with the +X side containing PMTs pointed away from the bulk of the spacecraft) was intended to reduce spacecraft background. See [1] for further details. Thermal control was facilitated by a radiator and heaters. The radiator, shown in Fig. 3A and 3B, was thermally isolated from the spacecraft with the outboard surface (white) exposed to space. The rest of the instrument was covered by MLI (not shown).

OPERATIONAL MODES

GRaND had three operational modes: 1) **STANDBY**; 2) **NORMAL**; and **ANNEAL**. The instrument started in STANDBY mode. In STANDBY mode, the radiation sensors were not operational (all commands were accepted except high voltage enable commands). Only SOH data were generated in standby mode. Data from the temperature sensors were recorded in STANDBY once the ±5V low voltage supply was activated. From STANDBY, the instrument could be commanded to NORMAL mode for which all commands were accepted. In NORMAL mode, the instrument could be configured for science data acquisition, including enabling and setting the high voltage level for each sensor. Both SOH and science data were included in the telemetry. From STANDBY, the instrument could also be commanded to ANNEAL mode, which was designed to anneal radiation damage accrued by the CZT crystals [1,15]. Only SOH data were generated in ANNEAL mode.
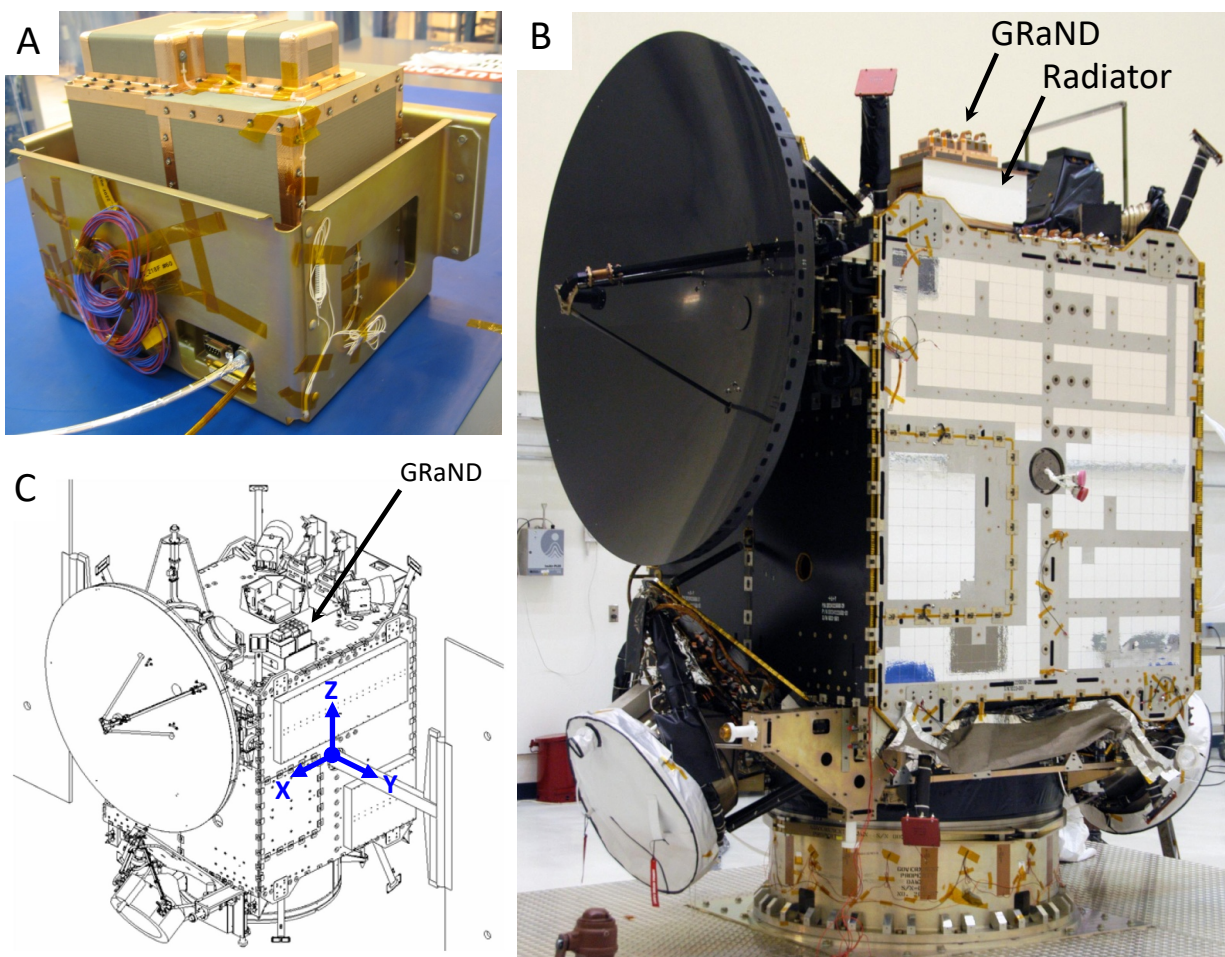
Figure 3. Accommodation of GRaND on the spacecraft. A) Instrument mounted in its radiator assembly and B) as installed on the spacecraft. C) Position and orientation of the instrument on the +Z deck of the spacecraft on the +Y side of the high gain antenna. Artwork adapted from [1].

MEASURED PARAMETERS

Each science record sent by GRaND contains counting data acquired during a collection interval, set by the commandable parameter **TELREADOUT**. State of health telemetry data were sampled and recorded in intervals of **TELSOH**, which was also commandable. The collection intervals were successive, forming a time series that can be analyzed to map elemental abundances. The records are time-tagged with the spacecraft clock (**SCLK**) value, input to NAIF/SPICE routines to determine spacecraft ephemerides and pointing for mapping. Each science record includes scaler data, event data, and histograms. The pattern of pulses recorded by the sensors for each radiation interaction was processed by the FPGA, which categorizes the events. The events were scaled and binned into histograms. In addition, a subset of neutron and gamma ray events were recorded in a fixed length list-mode buffer. At the end of each collection interval, the data were compressed, packetized, and transmitted. The event categories recorded by GRaND are as follows. Note that event categories 3, 5, 6, and 8 were deleted during instrument development. A diagram illustrating each of the event categories is provided in Fig. 4. Additional details can be found in [1].

Category 1 (CAT1): A single pulse from the -Z or +Z phoswich. CAT1 data were binned into a histogram (256 channels) which can be analyzed to determine the areas of peaks and 93 keV$_{ee}$ and 340 keV$_{ee}$ produced, respectively, by the $^{10}B(n,\alpha)$ and the $^{6}Li(n,t)$ reactions.

Category 2 (CAT2): A prompt coincidence between the BGO and any one of the phoswich or BLP scintillators. The pulse heights of the coincidence event must occur within windows, which weare set to bracket the 93 keV$_{ee}$ peak from the BLP/phoswich and the 478 keV full energy peak from the BGO. The upper and lower bounds of the windows were commandable. The CAT2 events were binned into histograms (64 channels), which can be analyzed to determine the flux of epithermal and thermal neutrons.

Category 4 (CAT4): A double-pulse occurring in any one of the phoswich or BLP scintillators. To reduce after-pulsing, events for which the second pulse occured within 400 ns of the first pulse were rejected. The maximum time to the second pulse (TTSP) recorded by GRaND was 25.6 microseconds. The amplitudes of the first and second pulse and the TTSP were recorded as event data in a fixed length buffer. The total number of CAT4 events processed by the FPGA during the collection interval was recorded in the scaler data. The CAT4 data can be analyzed to determine the flux and energy distribution of fast neutrons.

Category 7 (Cat7): A coincidence between a single CZT sensor and the BGO scintillator. The CZT pulse height (digitized by a 12-bit ADC) and CZT-sensor-ID were recorded as event data in the gamma event buffer. The BGO pulse height was recorded as a 9-bit unsigned integer. The portion of the gamma event buffer reserved for CAT7 events was commandable. The CAT7 data can be used to discriminate gamma rays originating from the target body and the spacecraft. For example, gamma rays originating from the target body can undergo low angle Compton scattering in a CZT sensor prior to entering the BGO crystal, where they may deposit the rest of their energy. The energy of the gamma ray can be determined by summing the pulse heights measured by the CZT and BGO sensors. Gamma rays originating from the spacecraft are shielded from the CZT array by the BGO crystal. In addition, those originating from the spacecraft that interact with a CZT sensor must scatter through a large angle, depositing a relatively large amount of energy in the CZT sensor before reaching the BGO crystal. Consequently, summing the energy deposited in the CZT and BGO sensors for events in which the energy deposited in the BGO sensor is greater than the energy deposited in the CZT sensor tends to reject gamma rays originating from the spacecraft.

Category 9 (CAT9): A single pulse from the BGO scintillator. The CAT9 events were binned into a 1024 bin histogram.

Category 10 (CAT10): A single interaction with a CZT sensor. The pulse height (digitized by a 12-bit ADC) and CZT-sensor-ID were recorded as event data in a fixed length buffer. The total number of CAT0 events processed by the FPGA during the collection interval was recorded in the scaler data. The CAT10 event data can be processed, given the known energy calibration for each of the sensors, to form a composite pulse height spectrum.

For data acquired in close proximity to Dawn's targets, the CAT9 histogram and CAT10 composite spectrum contain full energy peaks corresponding to radioactive decay and nuclear reactions occurring within the planetary surface, which can be analyzed to determine elemental abundances.

The scaler data provide additional information needed to analyze the histograms and event data, including a dead time counter. A scaler for events occurring in coincidence with three or more sensors (BGO and multiple BLP/phoswich) can be used as a galactic cosmic ray monitor.
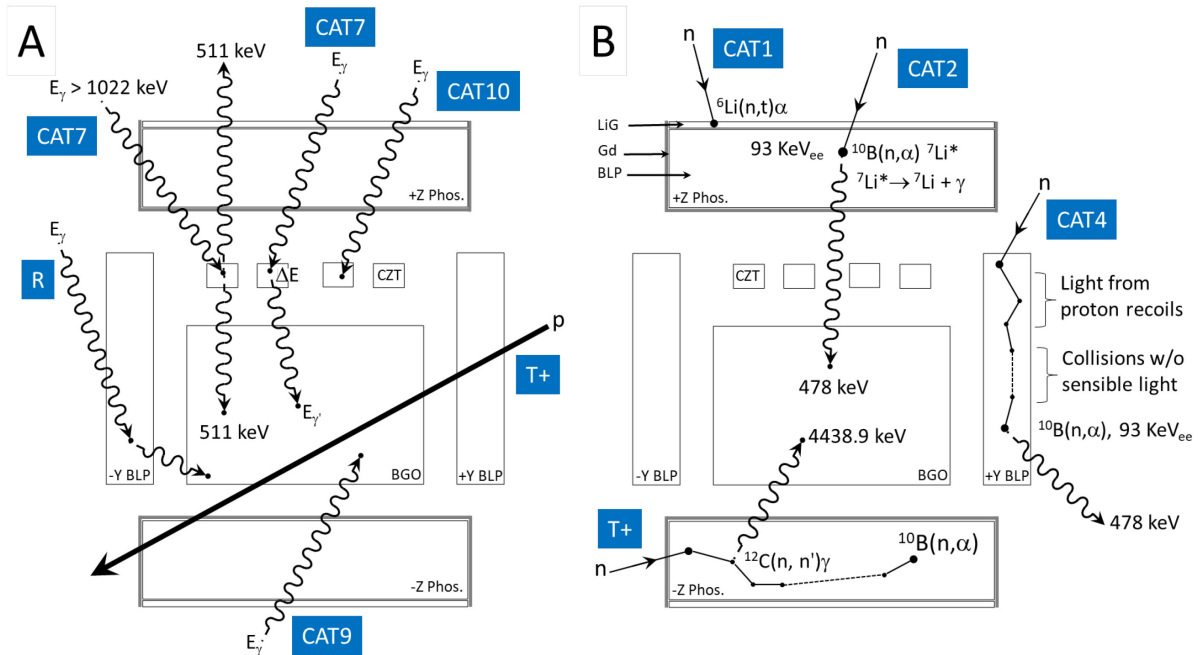
Figure 4. Illustration of **A**) gamma-ray and **B**) neutron events. The particle trajectories are superimposed on a Y-Z section of the sensors. **R** illustrates an event rejected by anticoincidence. Interactions marked **T+** are examples of events recorded by a three-or-more interactions (triples) scaler. Many of these events result from punch-through of high energy cosmic rays. Consequently, the triples+ counts was used as a proxy for the flux of galactic cosmic rays. Artwork adapted from [1].

TELEMETRY, DATA VOLUME, AND TIME

The telemetry for GRaND consisted of science and state-of-health data that were accumulated over commandable time intervals. Each science data record included scalers, histograms, and event data accumulated over an interval specified by the commandable parameter TELREADOUT (s). The state of health data included average temperatures, voltages, and instrument state data acquired during time intervals specified by the commandable parameter TELSOH (s). Both intervals are adjustable, depending on the measurement conditions and objectives for each mission phase. During mapping, TELREADOUT was be set to sub-sample spatial pixels defined on the surface of Vesta or Ceres. During cruise, TELREADOUT was generally set to large values (e.g., 210s) to minimize data volume. TELSOH is generally set to subsample the science accumulation interval, providing information needed to determine whether and how many times the science scalers have rolled over and information needed to precisely determine the start time of the science acquisition interval.

Onboard the spacecraft, the SOH and science data were stored in separate virtual recorders, VR3 and VR5, respectively. Prior to Mars Gravity Assist (MGA), the SOH data stored in VR3 were decimated. Consequently, the playback data from VR3 contain every third SOH packet. Real time data obtained while the spacecraft was in communication with a ground station are not decimated. Most of the data acquired during Initial Check Out (ICO) were in real time; however, only limited real time data are available afterwards. Prior to MGA, the decimation was removed and the playback data from VR3 contains a complete set of SOH data.

Table 1. List of data contained in each science record [1]. Note that while 24 scalars are listed, one of these is not used. Bits unaccounted for in this table include the packet headers for each of the 23 packets (14 bytes each) in the record and an additional 128 bytes that are not used. Note that all of the histograms were accumulated using 16-bit registers and were compressed to 8 bits/channel using the algorithm described by [16].

Data type (event category)	Number of items	Channels	Bits/channel	Total bytes
Scalars	24	1	16	48
Gamma ray and neutron event buffers (CAT4, 7, 10)	6676	3	8	20028
BGO histogram (CAT9)	1	1024	8	1024
±Z phoswich histograms (CAT1)	2	256	8	512
BGO-BLP coincidence (CAT2)				
BGO histograms	4	64	8	256
±Z phoswich histogram	2	64	8	128
±Y BLP histogram	2	64	8	128
			Total	22124

The telemetry rate for GRaND was determined by the selection of TELSOH and TELREADOUT. The SOH data were transmitted every TELSOH seconds in a single packet, 250 bytes in length. The science data were transmitted every TELREADOUT seconds in 23 packets containing a total of 22574 bytes, including packet headers and science data (see Table 1) Thus, the total telemetry rate was given by 8*(250/TELSOH+22574/TELREADOUT) bits per second, assuming no decimation of the SOH packets. For example, a typical telemetry rate for cruise (TELSOH=35 and TELREADOUT=210) was 917 bits per second. For Mars Closest Approach and during elliptical orbits in Ceres second extended mission (TELSOH=35 and TELREADOUT=35), the telemetry rate was 5217 bits per second.

Each science data packet was tagged with a SCLK value, which was derived from a timestamp command, sent by the S/C every 60s. The SCLK value stored in each science packet has a resolution of 1s and is updated at the time of transmission by the number of pulses from the S/C 1pps signal since the last timestamp. The 1pps signal had a dedicated line on the RS 422 interface and was monitored by the FPGA. GRaND's 1pps counter was reset only by the receipt of a timestamp command. So, the transmitted SCLK value was accurate to within 1s.

If the cadence of the science and SOH data were such that an SOH packet was sent during the transmission of science data, then the register in which the time stored was overwritten by the SCLK value from the last timestamp command. This resulted in "SCLK regression," for which science packets arranged by order of receipt by the ground station (or by packet sequence counter) were not ordered in time. SCLK regression resulted in the undesirable fragmentation of files in the Ground Data System.

The amount of time needed to transmit the science data at the end of each accumulation interval was 12s. So, to avoid SCLK regression, the SOH data need to be written at least 12s after the end of each science accumulation interval. This was accomplished by making TELREADOUT a multiple of TELSOH and starting the first SOH interval no more than TELSOH-12s before the start of the first science interval. Application of this procedure during flight was effective in eliminating instances of SCLK regression. Instances of SCLK regression affecting instrument occurred prior to Mars-Vesta cruise.

GRaND uses two memory locations to store science data such that data for the next accumulation interval can be acquired while data from the previous interval are being transmitted. Thus, TELREADOUT is an accurate measure

of the accumulation time. The dead time is recorded in the scaler data and is used to determine live time as discussed in the section on Level1b processing.

OPERATIONAL CONSIDERATIONS FOR SCIENCE DATA ACQUISITION

Science data was acquired by GRaND during Cruise, Mars Flyby, and while in orbit around Vesta and Ceres. To acquire the data, GRaND was placed in NORMAL mode with high voltages turned on and adjusted to nominal settings. Large gaps in the data occurred during cruise when the instrument was off. Data acquired within 1 body radius altitude with the instrument bore sight pointed close to body center are optimal for compositional analyses. To achieve ample sensitivity, long accumulation times under quiet Sun conditions are desired for which the interrogating source is primarily galactic cosmic rays. Solar activity resulting in energetic particle events can reduce the amount of data available for analyses.

REFERENCES

[1] Prettyman, T. H. *et al.* Dawn's gamma ray and neutron detector. *Space Science Reviews* **163**, 371-459, doi:10.1007/s11214-011-9862-0 (2011).

[2] Prettyman, T. H. *et al.* Elemental mapping by Dawn reveals exogenic H in Vesta's regolith. *Science* **338**, 242-246, doi:10.1126/science.1225354 (2012).

[3] Prettyman, T. H. *et al.* Neutron absorption constraints on the composition of 4 Vesta. *Meteoritics & Planetary Science* **48**, 2211-2236, doi:10.1111/maps.12244 (2013).

[4] Prettyman, T. H. *et al.* Concentrations of potassium and thorium within Vesta's regolith. *Icarus* **259**, 39-52, doi:10.1016/j.icarus.2015.05.035 (2015).

[5] Yamashita, N. *et al.* Distribution of iron on Vesta. *Meteoritics & Planetary Science* **48**, 2237-2251, doi:10.1111/maps.12139 (2013).

[6] Lawrence, D. J. *et al.* Constraints on Vesta's elemental composition: Fast neutron measurements by Dawn's gamma ray and neutron detector. *Meteorit Planet Sci* **48**, 2271-2288, doi:10.1111/maps.12187 (2013).

[7] Peplowski, P. N. *et al.* Compositional variability on the surface of 4 Vesta revealed through GRaND measurements of high-energy gamma rays. *Meteoritics & Planetary Science* **48**, 2252-2270, doi:10.1111/maps.12176 (2013).

[8] Prettyman, T. H. *et al.* Extensive water ice within Ceres' aqueously altered regolith: Evidence from nuclear spectroscopy. *Science* **355**, 55-59, doi:10.1126/science.aah6765 (2017).

[9] Lawrence, D. J. *et al.* Compositional variability on the surface of 1 Ceres revealed through GRaND measurements of high-energy gamma rays. **53**, 1805-1819, doi:doi:10.1111/maps.13124 (2018).

[10] Prettyman, T. H. *et al.* Elemental composition and mineralogy of Vesta and Ceres: Distribution and origins of hydrogen-bearing species. *Icarus* **318**, 42-55, doi:10.1016/j.icarus.2018.04.032 (2019).

[11] Prettyman, T. H., Englert, P. A. J. & Yamashita, N. Neutron, gamma-ray, and X-ray spectroscopy: Theory and applications in *Remote Compositional Analysis*   (eds J. L. Bishop, J. F. Bell, & J. E. Moersch) Ch. 9, 191-238 (Cambridge University Press, 2019).

[12] Prettyman, T. H., Englert, P. A. J., Yamashita, N. & Landis, M. E. Neutron, gamma-ray, and X-ray spectroscopy of planetary bodies in *Remote Compositional Analysis*   (eds J. L. Bishop, J. F. Bell, & J. E. Moersch) Ch. 30, 588-603 (Cambridge University Press, 2019).

[13] Prettyman, T. H. Remote Sensing of Chemical Elements Using Nuclear Spectroscopy in *Encyclopedia of the Solar System (Third Edition)* (eds Tilman Spohn, Torrence Johnson, & Doris Breuer) Ch. 54, 1161-1183 (Elsevier, 2014).

[14] Russell, C. T. *et al.* Dawn arrives at Ceres: Exploration of a small, volatile-rich world. *Science* **353**, 1008-1010, doi:10.1126/science.aaf4219 (2016).

[15] Prettyman, T. H. *et al.* Gamma-ray and neutron spectrometer for the Dawn mission to 1 Ceres and 4 Vesta. *IEEE Transactions on Nuclear Science* **50**, 1190-1197, doi:10.1109/tns.2003.815156 (2003).

[16] Feldman, W. C. *et al.* Gamma-ray, neutron, and alpha-particle spectrometers for the Lunar Prospector mission. *Journal of Geophysical Research* **109**, E07S06 (2004).